Pharmaceutical Research, Vol. 23, No. 9, September 2006 (© 2006)
DOI: 10.1007/s11095-006-9061-y

Research Paper

Pegylated Nanocapsules Produced by an Organic Solvent-Free Method: Evaluation of their Stealth Properties

Arnaud Béduneau,[1] Patrick Saulnier,[1,3] Nicolas Anton,[1] François Hindré,[1] Catherine Passirani,[1] Holisoa Rajerison,[2] Nicolas Noiret,[2] and Jean-Pierre Benoit[1]

Received February 24, 2006; accepted May 10, 2006; published online August 9, 2006

Purpose. To develop from an original process, a novel generation of stealth lipidic nanocapsules in order to improve the lipophilic drug delivery in accessible sites.
Materials and Methods. Nanocapsules covered by PEG_{1500} stearate were obtained by a low energy emulsification method. Conductivity measurements and ternary diagram were performed to describe the formulation mechanism. Hemolytic dosage CH50 and pharmacokinetic study in rats have been achieved in order to study the stealth properties of nanocapsules.
Results. Transition from an O/W emulsion to a w/O/W emulsion was necessary to produce PEG_{1500} stearate nanocapsules. Interestingly nanocapsules with a size around 26 nm and a polydispersity index inferior to 0.1 were obtained. The CH50 test has revealed a very weak complement consumption in the presence of such nanocapsules. Moreover, after intravenous injection into rats, PEG_{1500} stearate nanocapsules exhibited long circulating properties. The experimental data support the concept of steric repulsion of the surface towards proteins, displayed by nanocapsules covered with PEG_{1500} stearate. These *in vivo* results were in agreement with the PEG_{1500} density calculated at the nanocarrier surface.
Conclusions. Injectable drug carriers have been developed. Their long-circulating properties could confer them a strong potential for lipophilic drug targeting.

KEY WORDS: lipidic nanocapsules; PEG chain density; polyethylene glycol; "stealth" colloids; transitional inversion.

INTRODUCTION

For 40 years, drug carriers in the nanometer range have been in development. Most of them are used in the field of cancer therapy and diagnosis. Indeed, these submicronic systems, after intravenous administration, are expected to improve the targeting and release of the encapsulated drug. Liposomes and more recently, nanocapsules represent an important part of these carriers. They are composed of nonionic surfactants, macromolecules and / or phospholipids.

Unfortunately, following intravenous injection, these nanocarriers are rapidly cleared from the blood. Macrophages of the mononuclear phagocytic system, particularly Kuppfer cells in the liver, recognized and removed them from the bloodstream. The adsorption of plasma proteins at the surface of these particles (opsonization process) seems to be responsible of the short lifetime in the bloodstream because of their interaction with specific plasma membrane receptors on monocytes and various subsets of tissue macrophages (1). Therefore, to increase the circulating half-time of nanocarriers, some studies have shown the impact of grafting polyethylene-glycol (PEG) derivatives at their surface (2). Indeed, the presence of such polymers reduces the protein adsorption by ensuring an efficient steric stabilization. The PEG density, corona thickness and PEG chain length are important parameters to consider to avoid opsonization (3).

In this context, lipid nanocarriers covered with PEG_{660} hydroxystearate have been developed by Heurtault *et al.* (4) over the last five years. These standard nanocapsules were prepared according to an organic solvent-free process using the Phase Inversion Temperature (PIT) method (5). When an oil-in-water (O/W) emulsion prepared with a nonionic surfactant of the ethylene oxide type is heated to a critical temperature (PIT), the emulsion inverts to a water-in-oil emulsion (W/O) (6). During a rapid cooling at PIT, the system crosses a point of zero spontaneous curvature promoting the formation of submicron-scale particles. Despite of the presence of PEG, these lipid nanocapsules exhibit an early disappearance half-time of 21 min after injection in the bloodstream (7). In order to extend the disappearance half-time, a novel long-circulating particle with longer PEG chain (PEG_{1500} stearate) based on low-energy emulsification method, without phase inversion, was developed.

In this study, the formulation process of these nanocarriers was investigated. The nanocapsule structure was then explored by cryo-transmission electron microscopy (Cryo-TEM). The influence of the PEG length on the electrokinetic properties of the particles was compared to the standard nanocapsules developed by Heurtault *et al.* (8). The ability of the PEG_{1500}

[1] Inserm U646, Université d'Angers, Angers F-49100, France.
[2] UMR-CNRS 6052, ENSC, Rennes F-35700, France.
[3] To whom correspondence should be addressed. (e-mail: patrick.saulnier@univ-angers.fr)

stearate (density and length) to inhibit the *in vitro* activation of the complement system and to prolong the lifetime of the nanocapsules after intravenous injection in rats was also evaluated in comparison with PEG_{660} hydroxystearate nanocapsules.

MATERIALS AND METHODS

Lipoïd® S75-3 (soybean lecithin at 69% of phosphatidylcholine and 10% phosphatidylethanolamine) and DUB SPEG 30S® (PEG_{1500} stearate) were kind gifts from Lipoïd GmbH (Ludwigshafen, Germany) and Stearinerie Dubois (Citron, France), respectively. Due to its complex composition, the brand name of soybean lecithin will be used in the following. The lipophilic Labrafac® WL 1349 (caprylic-capric acid triglycerides) was generously provided by Gattefossé S.A. (Saint-Priest, France). NaCl was purchased from Prolabo (Fontenay-sous-bois, France). Deionised water was obtained from a Milli-Q plus® system (Millipore, Paris, France).

Formulation of Stearate PEG_{1500} Nanocapsules

An aqueous phase containing deionised water, NaCl, and hydrophilic non-ionic surfactant (DUB SPEG 30S®) was added to the oil phase (Labrafac®) and lecithin (Lipoïd®) (Table I under magnetic stirring at an agitation speed of 200 rpm. As for the preparation of standard nanocapsules, at least three temperature cycles alternating from 60 to 95°C at a rate of 4°C/min were realized to obtain stable nanocapsules (9). During the last cooling, the formulation reaching 80°C, was rapidly diluted (1:3.5) with 12.5 ml cold water to form particles, and then continuously stirred for 30 min.

Conductivity Measurement

The conductivity of the bulk phase was measured using a conductimeter LF 325B (WTW, Weilheim, Germany) with two platinum plate attachments. Conductivity was determined during heating, between 60 and 100°C, under magnetic stirring at an agitation speed of 200 rpm. The conductivimeter mode used was the nonlinear temperature compensation (nLF). Four different compositions corresponding to high, low and intermediate water fraction F_w (0.85, 0.66, 0.5 and 0.33) have been studied with F_w described as:

$$F_w = \frac{V_{water}}{(V_{water} + V_{oil})} \quad (1)$$

Where V_{water} and V_{oil} were the volumes of water and oil, respectively, in the nanocapsule suspension before dilution. Moreover, concentration of PEG_{1500} stearate was fixed at 30% w/w. The conductivity measurements were performed in triplicate indicating an accuracy around 1.5%.

Table I. Composition of PEG_{1500} Stearate Nanocapsules A

PEG_{1500} stearate nanocapsules (26 nm)	
Constituents	Quantity (g)
PEG_{1500} stearate	1.403
Lipoïd®	0.075
NaCl	0.250
Labrafac®	0.468
Deionized water	2.805
Deonized water at 0°C	12.50

Feasibility Domain

In order to optimize constituent proportions, a ternary diagram was built. For each plot, the preparation process was unchanged but the proportions of water, oil and PEG_{1500} stearate were modified. The sum of the amounts of these three components was considered to be 100% (w/w). Concentrations of Lipoïd® S75-3 and NaCl in water were fixed at 1.5% (w/w) and 5% (w/w), respectively. The feasibility domain was defined as an area that allowed the formation of nanocapsules. After dilution, the hydrodynamic diameter range and the polydispersity index of each formulation were characterized by dynamic light scattering spectroscopy.

Particle Characterization

Size Measurements

The average hydrodynamic diameter and the polydispersity index (PI) of nanocapsules were determined by dynamic light scattering using a Malvern Autosizer 4700 (Malvern Instruments S.A., Worcestershire, United Kingdom) fitted with a 488 nm laser beam at a fixed angle of 90°. The polydispersity index was used as a measurement of the size distribution. A small value of PI (< 0.1) indicates an unimodale size distribution, while a PI > 0.3 indicates a higher heterogeneity. The temperature of the cell was maintained at 25°C. Nanocapsules were diluted 1:100 (v/v) in deionised water in order to assure a convenient scattered intensity on the detector.

Cryo Transmission Electron Microscopy (Cryo-TEM)

Cryo-TEM observations were performed at −170°C on a Philips CM120 electron microscope operating at −120 kV following the method previously developed by Lambert *et al.* (10).

Determination of the Proportion of Free PEG_{1500} Stearate in the Nanocapsule Suspension

We assumed that the whole quantity of Labrafac® and Lipoïd® used in the preparation was confined into spherical particles. On the contrary, a release of the PEG_{1500} stearate from the nanocapsule shell has been noticed. So, an assessment of PEG_{1500} stearate amount in the external phase of the suspension was performed. The free hydrophilic polymer was separated from the nanocapsules by steric exclusion chromatography. Nanocapsule suspension was deposited on 1.5 × 40 cm Sepharose CL-4B column and was eluted with distilled water. About 200 fractions of 400 µl were successively collected and the PEG concentration was determined from a colorimetric method taking advantage of the formation of a complex between PEG and iodine (11). 50 µl of KI/I_2 solution was added to 100 µl of sample diluted at 1:4 (v/v) and the turbidity of the medium was then detected spectrophotometrically at 492 nm. Three measurements by fraction were performed to evaluate the PEG concentration indicating a 1% accuracy. After chromatography, the amount of PEG_{1500} stearate adsorbed on the Sepharose gel was determined according to the same method.

Measurement of the Electrophoretic Mobility

Electrophoretic mobility measurements of nanocapsules were carried out using a Zetasizer 2000, (Malvern Instruments S.A.) based on the laser Doppler effect. Measurements were made in water at pH 7.4 with cell voltage 150 V. The nanocarriers were diluted in water at 1:10 (w/w) and seven NaCl concentrations were chosen: 1, 2, 10,15, 25, 50 and 100 mM. The electrophoretic mobility measurements were carried out in triplicate. All the values were measured with a relative accuracy of 1%.

From these experimental electrophoretic mobilities, a soft particle analysis theory (12) was applied. It aimed at characterizing the surface electric properties of PEG_{1500} stearate nanocapsules (13). Two physical constants ZN and $1/\lambda$ were then determined: ZN ($C.m^3$) represented spatial charge density in the polyelectrolyte region and λ^{-1} (m) was the depth of the layer accessible by counterions like Na^+.

Complement Consumption Studies

Complement consumption was assessed in human serum (HS) by measuring the residual hemolytic capacity of the complement system after contact with nanocapsules. Various amounts of the nanocapsule suspension (50,100, 125, 150, 200, 250 µl) were diluted with VBS^{2+} (Veronal Buffer Saline) in order to obtain a total volume of 300 µl for each sample. After addition of 100 µl of HS, the suspensions were incubated at 37°C for 60 min, under gentle agitation. Simultaneously, sheep erythrocytes were sensitized with hemolysine diluted at 1:1,600 (v/v) in VBS^{2+} and suspended to a final concentration of 1.10^8 cells/ml. After incubation, nanocapsules in HS were diluted to 1:24 (v/v) and different amounts of the mixture nanocapsules/serum (0.2, 0.25, 0.3, 0.35, 0.4, 0.6 ml) were diluted with VBS^{2+} to reach a total volume of 0.8 ml. The sensitized sheep erythrocytes (0.2 ml) were also added and the sample were incubated at 37°C for 45 min. After addition of 2 ml of NaCl, unlysed erythrocytes were separated by centrifugation. The lysis of cells measured at 405 nm allowed to determine the level of residual active complement in HS previously exposed to nanocapsules. Zymosan particles, a strong complement activator (14), were used as a positive control. Results were expressed as CH50 units consumption (15). The CH50 units represent the concentration of serum of hemolytic complement units per ml of serum able to cause 50% hemolysis of a fixed volume of these sheep red cells.

***In Vivo* Studies**

Preparation of Radiolabeled Nanocapsules

Nanocapsules were labeled by incorporating in their oily core a lipophilic complex: ^{99m}Tc $(S_3CPh)_2(S_2CPh)$ or ^{99m}Tc-SSS complex, prepared according to Mevellec *et al.* (16). ^{99m}Tc was obtained from a $^{99}Mo/^{99m}Tc$ generator purchased from CIS bio International/Schering (Gif sur Yvette, France). 1 ml of deionised water was added to a vial containing 7.5 mg sodium gluconate and 0.075 mg $SnCl_2.2H_2O$ in a freeze-dried form. Pertechnetate (370 Mbq, 0.5 ml) was mixed with this solution at room temperature for 10 min. 4 mg of a sodium dithiobenzoate and trithiobenzoate mixture in 0.5 ml of deionised water were finally added and heated for 30 min at 100°C. The radiochemical purity of the lipophilic complex was determined by thin layer chromatography and the migration was evaluated using a phospho-imager apparatus (Packard, Cyclone™ storage phosphor system). The chromatography was carried out on silica/alumina 60 F_{254} gel plates (Merck), using a solution of petroleum (6/4) as eluant (Rf 0.7). PEG_{1500} stearate nanocapsules were prepared in adding ^{99m}Tc-SSS complex to the raw materials. Its volume was deduced of the total amount of deionised water before dilution. The rest of the preparation process previously described remained then unchanged. The nanocapsules were finally dialyzed against distilled water (2 l), at room temperature during 2 h.

Animal Experimentation

Animal studies were carried out in accordance with the French regulation (law 0189.4 of January 24, 1990) on male Wistar rats (400–450 g). The ^{99m}Tc nanocapsules (500 µl, 0.2 MBq) were injected intravenously in the penile vein under gaseous isoflurane anesthesia. Blood samples (0.5 ml) were withdrawn on four animals intracardially at 15, 45, 90 min, 2, 4, 6, 16, 24, 41 and 48 h after injection. They were then introduced into vials, weighted and counted in a gamma counter (Packard Auto-Gamma 5000 series) for activity. Nanocapsule concentrations in blood at the various time points were calculated based on the assumption that blood represents 7% of rat body weight and were expressed as percent of the injected dose.

Data Analysis

The pharmacokinetic data were analyzed by a non-compartmental analysis. The time corresponding to the disappearance of 50% of the total injected dose was determined by linear interpolation. The $AUC_{[0-24]}$ and $AUC_{[0-48]}$ calculations were performed by the trapezoidal method during the experimental period.

RESULTS AND DISCUSSION

Conductivity Measurements

The conductivity study was performed on four formulations containing a constant PEG_{1500} stearate concentration (30% w/w) and different F_w. The conductivity evolutions were determined under magnetic stirring while the temperature was increased. Two different behaviors were observed for systems with high and low water proportions. In order to describe these profiles, two representative preparations (Table II) among the four were chosen: the formulation A ($F_w = 0.85$) and the formulation B ($F_w = 0.5$).

The conductivity of the system A as a function of the temperature was exhibited in Fig. 1A. A constant conductivity around 33 mS/cm corresponding to a O/W emulsion was observed until 76°C. Then, the conductivity exhibited a variation zone between 76 and 90°C to attain afterwards a threshold value of 29 mS/cm. This significant conductivity above 90°C denoted an aqueous external phase. So, this behavior was not suggestive of a phase inversion but of a transition from a O/W emulsion to a w/O/W emulsion (17) by

Table II. Composition of Preparations Used for Conductivity Studies

Quantity (g)	Formulation A	Formulation B
PEG_{1500} stearate	28.05	28.05
Lipoïd®	1.5	1.5
NaCl	5	2.92
Labrafac®	9.35	32.73
Deionized water	56.1	32.73

The water fractions (F_w) for formulations A and B were 0.85 and 0.5, respectively. For each preparation, the NaCl concentration in aqueous phase was constant (89 g/l).

passing through a transitional zone characterized by conductivity changes (in gray on the graph). The proportion of inner water ($F_{w_{in}}$) contained in the multiple emulsion was calculated from the difference between the experimental conductivity and the expected one predicted by Bruggeman's law described below:

$$\kappa = \kappa_w \times F_W^{3/2} \quad (2)$$

Where κ was the emulsion conductivity and κ_w, the aqueous phase conductivity with the same NaCl concentration. For temperatures below 76°C corresponding to a O/W emulsion, this equation was applied. The experimental conductivity was around 33 mS/cm and the conductivity calculated from Bruggeman's law was 33.7 mS/cm with κ_w = 43 mS/cm. On the contrary, after the transitional zone, the conductivity measured (29 mS/cm) was lower than the one determined from Bruggeman's law suggesting the presence of water within the oil drops. The inner water amount was determined from these conductivity differences to be about 8% (w/w) and the total internal phase of the w/O/W emulsion was around 25% (w/w).

The conductivity of the composition B containing equal amount of oil and water (F_w = 0.5) is illustrated in Fig. 1B. As in the case of the system A, the conductivity stayed constant (i.e., 8.5 mS/cm) for temperatures below 75°C. This conductivity value was in agreement with the one determined with the Bruggeman's equation (i.e., 8.1 mS/cm with κ_w = 23 mS/cm). Between 75 and 95°C, a rapid conductivity decrease was observed until 0 mS/cm corresponding to an external phase inversion. Indeed, during the temperature increase, the inner oil phase moved to the external phase in crossing a transitional zone and the O/W emulsion became a W/O emulsion. This behavior is representative of classical PIT method used by Heurtault *et al.* (9).

The conductivity changes observed for each formulation occurred at the same range of temperature, between 75 and 90°C into a transitional zone corresponding to the gray region in Fig. 2. For emulsions composed of 30 to 65% of water, the interfacial curvature was inverted with temperature increase according to the Bancroft's rules (18) while crossing the transitional zone. Phase inversion was not possible for systems with higher water fraction because the oil amount is too small, and their interfacial curvature is opposite to the one naturally induced by the non-ionic surfactant leading to multiple emulsion w/O/W (19). During the temperature cycles, these morphology changes were due to the variation of surfactant affinity for aqueous and oily phases defined by an empirical formulation variable so-called the hydrophilic–lipophilic deviation (HLD). HLD > 0 and HLD < 0 correspond to surfactant affinity for oil and for water, respectively (20). A HLD value equal to 0 represents an optimum formulation where an uniform repartition of surfactant between the two phases occurs. A formulation-composition map introduced 20 years ago described the variations of the emulsion morphology according to the water fraction F_w and the HLD (21). Thus, making a correlation between this map and the Fig. 2, we hypothesized that the transitional zone corresponds to the optimum formulation of system with a HLD value close to 0. In this narrow domain, the spontaneous curvature of the PEG_{1500} stearate is near zero leading to the disappearance of droplets (22). Then, a bicontinuous microemulsion phase with excess water and/or oil takes place (23).

After three temperature cycles, the preparations A and B were diluted with cold water and were analyzed by photon correlation spectroscopy (PCS). Some nanocapsules exhibiting a small hydrodynamic diameter (26 nm) and a monomodal distribution (PI < 0.1) were produced from the composition A. On the contrary, despite of the inversion phase observed during the temperature increase, no structure

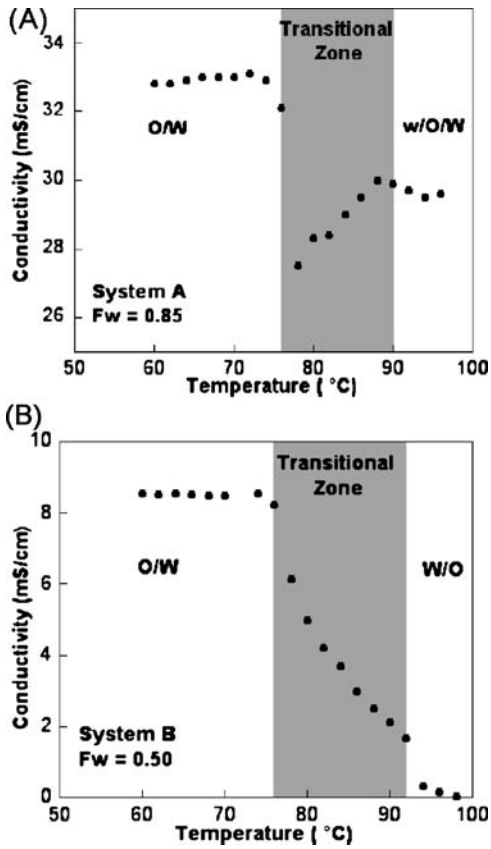

Fig. 1. Evolution of the conductivity as the temperature increases. The PEG_{1500} stearate concentration was 30% (w/w). The conductivity variations occurred in the transitional zone represented in gray on the graphics. (A) For the system A composed of a water fraction (F_w) of 0.85, the crossing of the *gray zone* corresponded to a transition from a O/W emulsion to a multiple w/O/W emulsion. (B) For system with a lower water fraction (F_w = 0.5), the conductivity when temperature increased, sharply decreased up to 0 mS/cm denoting a phase inversion.

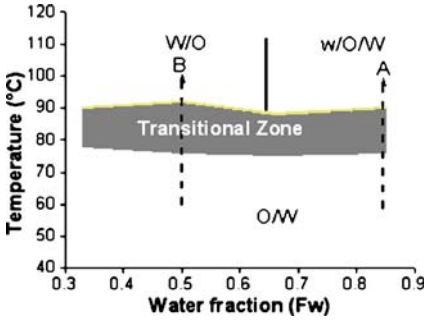

Fig. 2. Morphology evolutions as a function of temperature for four systems containing 30% (w/w) of PEG_{1500} stearate and different water fractions: F_w = 0.33; 0.5; 0.66; 0.85. Transitional zone (*in gray on the graphic*) represented conductivity variations denoting a morphology change. For preparations composed of high water fractions ($F_w > 0.6$), temperature increase led to a transition from a O/W emulsion to a multiple w/O/W emulsion. For systems with lower water proportions, phase inversion took place in the transitional zone.

was obtained for the formulation B. These results could be correlated with the work of Wadle *et al.* (24) who had demonstrated that the occurrence of phase inversion was not a guaranty of the nanocapsule formation. Moreover, according to Morales *et al.* (25), the preparation of nano-emulsion implies a complete solubilization of the oil phase in a bicontinuous microemulsion, at PIT. Thus, we could suppose that for low F_w inducing phase inversion during temperature cycles, the oil is not entirely soluble. Concerning the standard nanocapsules developed by Heurtault *et al.*, their preparation required the crossing of a phase inversion zone between 70 and 85°C (9). These formulations composed of PEG_{660} hydroxystearate were characterized by lower water fractions leading to phase changes (8). Hence, for these systems, a significant oil solubilization occurs within the bicontinuous microemulsion.

Feasibility Domain

A ternary diagram was established to define the constituents proportions of salted water, Labrafac® and PEG_{1500} stearate allowing the formation of submicron particles with a monodisperse size distribution. The formulation process, previously described, was applied for each point of the diagram (Fig. 3). Particle size and distribution were then determined for each formulation. A feasibility domain, in gray on the graphic, corresponding to the formation of nanocapsules with a size comprised between 20 and 150 nm and an polydispersity index inferior to 0.3 was revealed. It is described as a parallelogram whose relative proportions are comprised between 20 and 40% (w/w) of non-ionic surfactant, 40 and 75% (w/w) of salted water and 5 and 20% of Labrafac®. Furthermore, as in the case of system A, we noticed that the particle formation occurred only at F_w above 0.65. Thus, we could suppose that for all the systems within the feasibility domain, the process of particle formation is similar to the one occurring during the preparation of A: no phase inversion but a transition from a W/O emulsion to a w/O/W emulsion by passing through a zone corresponding to a bicontinuous phase allowing the formation of nanocapsules.

In conclusion, the complete process leading to the nanocapsule formation is illustrated in Fig. 4, where the morphology changes of systems occurring during the temperature cycle is exhibited. A transition from a O/W emulsion into a w/O/W is induced when the temperature is increased to 95°C and vice-versa. Three temperature cycles were applied and a rapid cooling was performed inside the transitional zone.

The previously mentioned system (A) was subjected to Cryo-TEM observation (Fig. 5). The capsules analyzed by using electron beam at different angles (results not shown) were spherical. The size observed was around 25 nm, similarly to the hydrodynamic diameter determined by PCS (26 nm). The narrow size distribution characterized by both Cryo-TEM and PCS (PI < 0.1) contributed to improve the stability of the suspension by reducing the Ostwald ripening (6). This hypothesis was confirmed by macroscopic observations at 4 and 37°C and at different pH (6, 7.4 and 8) showing a stability of the suspension over three months.

The next studies have been carried out on the system A which exhibited a monomodal granulometric distribution and an interesting size (26 nm) for drug delivery. Each experiment was performed immediately after the preparation of nanocapsules.

Influence of the PEG_{1500} Stearate on the Stealthiness of Nanocapsules

The capacity of PEG_{1500} stearate into the nanocapsule shell to reduce complement consumption has been exhibited in Fig. 6. The results were then compared to a previous study of Vonarbourg *et al.* (26) concerning the evaluation of the complement activation by 50 nm PEG_{660} hydroxystearate nanocapsules. Complement activation expressed as CH50 units consumption was evaluated as the residual lytic capacity of the serum after contact with nanocapsules. A strong complement activation occurred in the presence of very small amount of Zymosan particles. On the contrary, nanocapsules did not induce any response of the complement

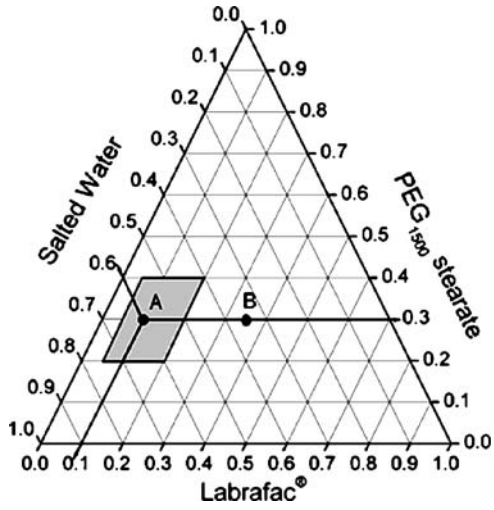

Fig. 3. Ternary diagram allowing the determination of feasibility domain comprising nanocapsules with a size smaller than 150 nm and a polydispersity index inferior to 0.3. The composition A characterized by a water fraction F_w = 0.85, led to the formation of nanocapsules with a size around 26 nm and a monomodal distribution. On the contrary, the formulation B composed of a lower water amount (F_w = 0.5) was located outside of the feasibility domain.

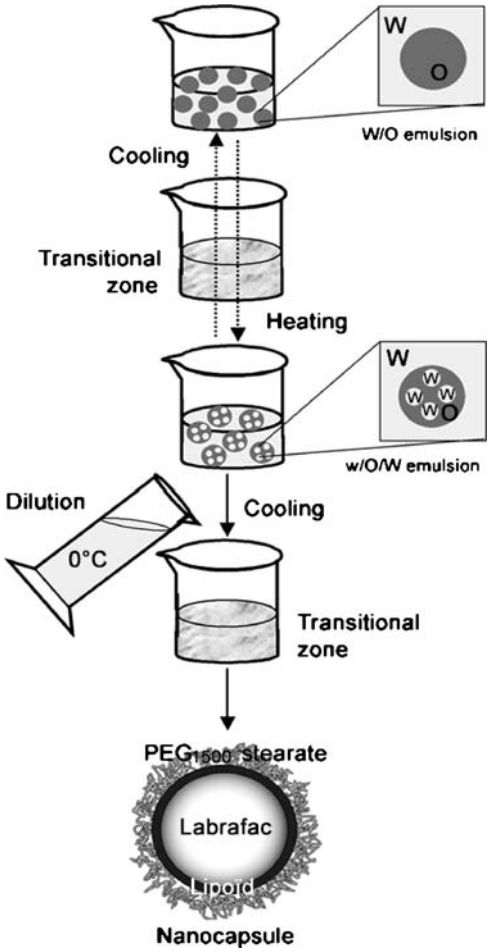

Fig. 4. Formulation process of lipid nanocapsules composed of a high water fraction and description of morphology changes during the temperature cycles.

system for a surface area lower than 1,000 cm^2. For higher surface area, between 2,000 and 5,000 cm^2, the complement consumption took place reaching a maximum of 20% and 15% for PEG_{1500} stearate and PEG_{660} hydroxystearate nanocapsules, respectively. This very weak complement activation observed for each type of nanocapsules was mainly due to the synergistic effect between the nanocapsule size and PEG layer. Indeed, the complement cascade involving a chain reaction of several complement components requires a certain local area on the nanocapsule surface. Ishida *et al.* (27) reported that the surface area of liposomes recognized by complement surface (SRC) was proportional to their diameter. Thus, the small size of nanocapsules limits the recognition of complement system (28). In addition to the size, the PEG layer surrounding the particle plays a major role in the weak complement activation observed in this study. The steric repulsion exerted by the PEG reduces adsorption of complement fragments (29). This protein-resistant effect was dependent on both polymer chain length and polymer surface density (1). However, Jeon *et al.* (30) demonstrated that the PEG surface density had a greater effect than length on steric repulsion.

In this context, the stearate PEG_{1500} density at the surface of nanocapsules has been assessed. The method used

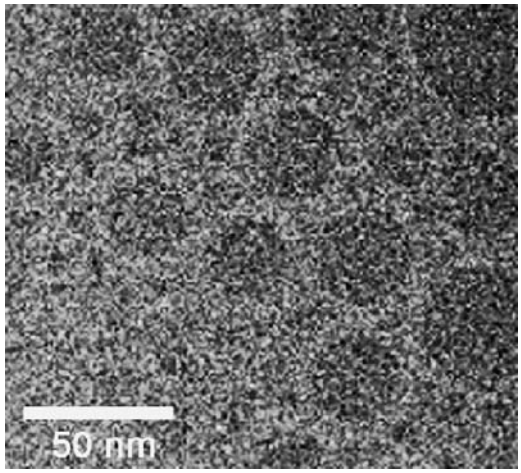

Fig. 5. Cryo-TEM image of nanocapsules A.

to evaluate the number of nanocapsules by volume unit (N_{caps}) has been developed by Minkov *et al.* (31) and was applied to PEG_{660} hydroxystearate nanocapsules. The authors hypothesized that the thickness of the particle shell was mainly influenced by the Lipoid® and corresponded to a 4.5 nm bilayer membrane. As a consequence, the shell thickness of 26 nm nanocapsules was estimated to about 4.5 nm and the diameter of the Labrafac® core (d) to about 17 nm. Moreover, the free PEG_{1500} stearate contained in suspension was separated by Sepharose CL-4B column chromatography. Its assessment was performed by a colorimetric method. Two peaks were observed from the chromatogram in Fig. 7, the nanocapsules were first eluted, their diameter analyzed by dynamic light scattering was about 30 nm. The free PEG_{1500} stearate corresponding to the second peak was composed of 43% (w/w) of the total amount of PEG contained in the nanoparticle suspension. Moreover, a negligible amount of PEG_{1500} adsorbed on the Sepharose gel was determined after chromatography. Thus, we could consider that the nanocapsule shell contained 57% (w/w) of the total PEG_{1500} stearate amount incorporated in the formulation. From this value ($P_{st\ PEG1500} = 0.57$) and the other approximations, the surface of one PEG_{1500} stearate molecule confined into the nanocapsule corona ($S_{st\ PEG1500}$) was calculated by the following equation:

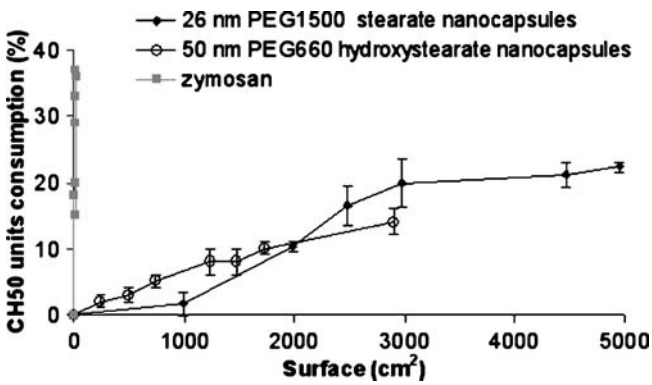

Fig. 6. Consumption of CH 50 units in the presence of 26 nm PEG_{1500} stearate nanocapsules A , 50 nm PEG_{660} hydroxystearate nanocapsules and Zymosan particles as function of surface area.

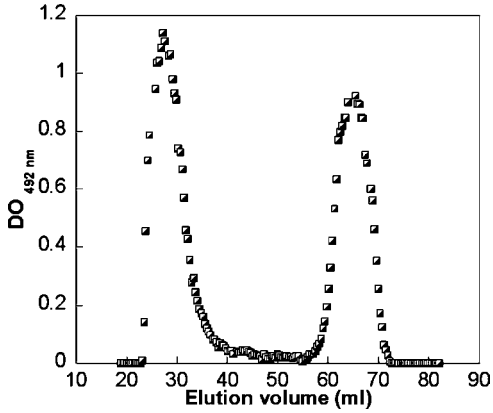

Fig. 7. Elution profile of PEG_{1500} stearate nanocapsules A obtained by Sepharose CL-4B gel filtration chromatography. The first peak corresponded to nanocapsules and the second one to free PEG_{1500} stearate.

$$S_{\text{st PEG1500}} = \frac{(N_{\text{caps}} \times S_{\text{caps}})}{(N_{\text{st PEG1500}} \times P_{\text{st PEG1500}})} \quad (3)$$

Where $N_{\text{st PEG1500}}$ was the total number of PEG_{1500} stearate molecules per unit volume in the preparation, $P_{\text{st PEG1500}}$ was the proportion of surfactant molecules in the nanocapsule shell, S_{caps} was the surface area of one nanocapsule and N_{caps} was the number of nanocapsules per unit volume, N_{caps} was given by:

$$N_{\text{caps}} = \frac{N_{\text{lab}}}{n_{\text{lab}}} \quad (4)$$

Where N_{lab} was the total number of Labrafac® molecules per unit volume and n_{lab} was the number of Labrafac® molecules confined in the nanocapsule core, n_{lab} was given by:

$$n_{\text{lab}} = \frac{V_{\text{core}}}{V_{\text{lab}}} \quad (5)$$

Where V_{core} was the volume of the Labrafac® core and V_{lab} (32,33) was the volume of one Labrafac® molecule. The numerical data used:

$P_{\text{st PEG1500}} = 0.57$
$N_{\text{st PEG1500}} = 2.7 \times 10^{19}$
$S_{\text{caps}} = 2124\ \text{nm}^2$
$N_{\text{lab}} = 3.4 \times 10^{19}$
$V_{\text{core}} = 2572\ \text{nm}^3$
$V_{\text{lab}} = 1.54\ \text{nm}^3$

The surface covered by one molecule of PEG_{1500} stearate was then estimated to about 2.8 nm^2, corresponding to a distance D between two PEG chains of about 1.7 nm. From previous studies about interactions between protein adsorption and PEG density, the polymer surface density is believed to be sufficient to prevent the opsonization process. Indeed, Jeon *et al.* (30) demonstrated that $D = 1$ nm and $D = 1.5$ nm were the optimal distances to prevent the adsorption of small and large proteins, respectively. Furthermore, Gref *et al.* (3) have shown that nanospheres made from copolymer block PEG-PLA allowed a maximum protein repelling when $D = 1.4$ nm. A weak complement consumption has been obtained for nanocapsules possessing on their surface some PEG chains separated by a distance D of about 2 nm (34). Therefore, these results are in agreement with previous assessments of the complement consumption. Indeed, the complement system was weakly activated by the nanocapsules because of the optimal PEG_{1500} stearate density surface which prevented the adsorption of complement protein fragments. The presence of such a surfactant strongly reduced Van Der Vaals forces and increased steric repulsion between particles and proteins. Concerning the standard nanocapsules, the PEG density has not been assessed. However, Vonarbourg *et al.* (35) showed that PEG_{660} hydroxystearate was organized in brush conformation suggesting a high PEG density on the particle surface.

The electrokinetic properties of the PEG_{1500} stearate nanocapsules have also been assessed from a soft particle electrophoresis analysis (12). The electrophoretic mobilities of nanocapsules as a function of the salt concentration were observed in Fig. 8. The best fit between experimental points and those corresponding to the theoretical model was obtained when ZN = -1.12×10^6 C.m^{-3} and $\lambda^{-1} = 1.0 \times 10^{-9}$ m with $R^2 = 0.97$. ZN corresponded to spatial charge density and λ^{-1} represented the depth of the layer accessible to the counterions. The correlation coefficient > 0.95 proved that nanocapsules verified the theory of soft particle. These results have been compared to the values obtained for standard lipid nanocapsules (LNC) with PEG_{660} hydroxystearate and the same Lipoïd® amount (Table III). We noticed that the charge density of PEG_{1500} stearate nanocapsules was three-fold higher than LNC. Vonarbourg *et al.* (35) demonstrated that PEG chains own negative dipolar charges playing a major role in the particle electrokinetic properties. So, this important ZN value could explain a higher PEG_{1500} stearate density into the nanocapsule shell. Furthermore, in spite of the longer PEG chain, the thickness of the accessible layer to Na^+ ions was thinner for PEG_{1500} nanocapsules than for LNC. We could hypothesize that λ^{-1} was weaker because of the short distance between two polymer chains, preventing the penetration of counterions into the accessible layer. In consequence, both ZN and λ^{-1} suggest, as the previous study, a high PEG_{1500} stearate density at the nanocapsule surface.

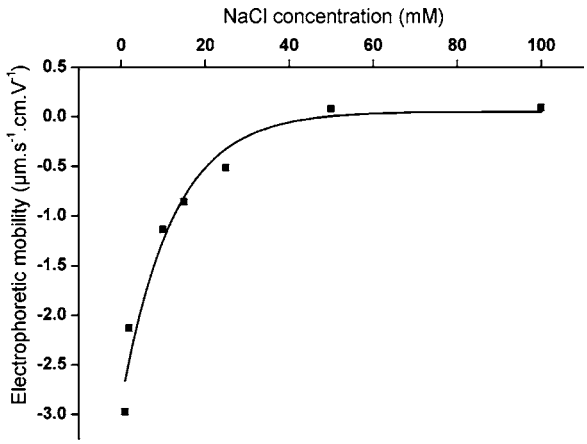

Fig. 8. Evolution of the electrophoretic mobility as a function of NaCl concentration for PEG_{1500} stearate nanocapsules A.

In a last part, the PEG_{1500} stearate nanocapsule pharmacokinetics were investigated in healthy rats in order to study the correlation between the low complement consumption by the particles and their circulation time in the bloodstream. The nanocapsule concentration in the bloodstream was determined *versus* time (Fig. 9). The results were compared to a pharmacokinetic study realized on standard ^{99m}Tc-labelled nanocapsules (7). The free ^{99m}Tc-SSS complex in the suspension was previously removed by dialysis. The half disappearance time of PEG1500 stearate nanocapsules was observed around 5.5 h. Moreover, 20% of the dose was still present in the blood 24 h after injection. These pharmacokinetic characteristics are more advantageous in comparison with standard LNC. Indeed, Ballot *et al.* demonstrated the rapid clearance from blood of nanocarriers composed of PEG_{660} hydroxystearate with a $t_{1/2}$ of 21 min. Although these capsules activate very weakly the complement system, they are rapidly recognized by the reticulo-endothelial system (RES) organs. These results could be explained by the change of physicochemical properties of standard nanocapsules after their intravenous administration. Indeed, we could hypothesize a possible leakage of PEG_{660} hydroxystearate from shell and / or a modification of the surfactant organization after injection in the blood. Moreover, by grafting DSPE-PEG_{2000} and DSPE-PEG_{5000} on the surface of these nanocapsules, Hoarau *et al.* (2) showed a significant improvement of their circulation time. This pharmacokinetic behavior was due to the length of PEG chains which reduced protein adsorption (36). Gref *et al.* (37) reported that the blood circulation time for nanospheres composed of PLA-PEG copolymers was significantly improved with increasing of molecular weight of PEG chains. Nevertheless, although the nanocapsules modified by Hoarau *et al.* were composed of PEG chains with a molecular weight superior to 1,500 g/mol, their $AUC_{[0-24]\ blood}$ (796%dose.h) corresponded to only 75% of that of PEG_{1500} stearate nanocapsules (1,053% dose.h). So, this difference suggested that the protein-resistant effect of the PEG density was greater than the length of the polymer chain. Moreover, this experiment allowed to correlate the low complement activation by the nanocapsules with their long-circulating properties. Indeed, by reducing the complement proteins consumption, the injected nanocapsules were not rapidly recognized by macrophages, increasing their residence time in the bloodstream (38,39). Thus, decreasing the recognition by complement system, the PEG density and the size of colloids represent essential parameters to confer stealth properties to particles. Nevertheless, an other parameter, the lecithin presence, could be taken into account. Mosqueira *et al.* (40) has compared nanocapsules composed of PLA-$PEG_{20\ 000}$ copolymers and of lecithin with nanospheres without phospholipids and characterized by a higher

Table III. ZN and $1/\lambda$ Parameters for Classic Lipid Nanocapsules Prepared with PEG_{660} Hydroxystearate and Novel Nanocapsules A Composed of PEG_{1500} Stearate

Type of LNC	ZN (10^6 c.m^{-3})	$1/\lambda$ (10^{-9} m)	R^2
PEG_{660} nanocapsules 20 nm	−0.32 ± 0.08	2.5 ± 0.5	0.99
PEG_{1500} nanocapsules 26 nm	−1.12 ± 0.08	1 ± 0.5	0.97

R^2 corresponded to the correlation coefficient obtained from the fitting.

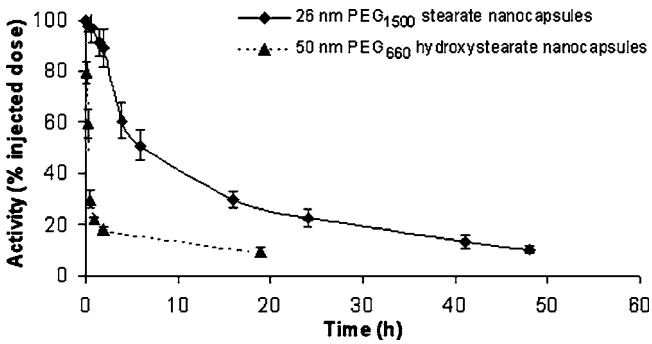

Fig. 9. Blood concentration-time profile for PEG_{1500} stearate nanocapsule A. Formulation was intravenously injected at a dose of 500 µl nanocapsules/rat and evolution of blood activity was expressed in percentage of injected dose. The results were compared to 50 nm PEG_{660} hydroxystearate nanocapsules.

PLA-$PEG_{20\ 000}$ density. The results showed that liver association of nanocapsules was 2- to 3-fold lower for nanocapsules in spite of their low PEG density. The authors have explained this phenomenon by the presence of lecithin that confers hydrophilic properties to the nanocapsule surface. Indeed, hydrophilic coating is known to decrease the opsonization process (41). However, their $AUC_{[0-24]\ blood}$ was sharply lower in comparison with PEG_{1500} nanocapsules (190%dose.h) probably due to their larger size (197 nm). Consequently, the Lipoïd® inside the PEG_{1500} stearate shell could contribute to long-circulating properties. Furthermore, the lipidic nanocapsules show an other advantage for lipophilic drug delivery in comparison with submicron lipid emulsions. Lundberg *et al.* (42) reported that the rapid clearance of 44 nm nanoemulsion composed of triolein (TO), dipalmitoyl phosphatidylcholine (DPPC) and polyethylene glycol modified phosphatidylethalonamine (PEG-PEG) was mainly due to the lypolis of the TO and not by uptake of whole emulsion droplets. In our case, the enzymatic degradation of nanocapsules was prevented by the polymeric shell protecting the oily core.

CONCLUSIONS

In this study, we have developed a new generation of nanocapsules composed of an oily core surrounded by a PEG_{1500} stearate layer with phospholipids and where no coating was necessary to make them stealthy. Their preparation did not allow the crossing of an inversion zone as in the case of the PIT method, but a transition from a O/W emulsion into a w/O/W multiple emulsion. *In vitro* and *in vivo* studies have revealed the long-circulating properties of these novel nanocapsules. Indeed, the complement system playing a major role in phagocytosis of colloidal drug carriers was only slightly activated in the presence of nanocapsules. This *in vitro* behavior also corroborated *in vivo* results. When nanocarriers were injected intravenously to rats, 20% of the total dose was still in the bloodstream 24 h after administration. Hence, we could suppose that these capsules prevented the opsonization process, consequently reducing their uptake by the mononuclear phagocytic system. The optimal protein-resistant effect of PEG_{1500} stearate on nanocapsule surfaces was considered to be dependent on both chain length and surface density. The PEG_{1500} stearate density calculated on

the nanocapsule surface was consistent with the literature findings. Indeed, the distance of 1.7 m between each PEG chain corresponded to a threshold value for optimal protein resistance. Moreover, the small size (26 nm) and the presence of lecithin on the nanocapsule surface contribute also to their stealth properties.

So, these PEG_{1500} stearate nanocapsules characterized by long-circulating properties allowed a potential application for delivery of lipophilic drugs to solid tumors. Indeed, contrary to the standard colloidal carriers that were rapidly recognized by macrophages, the stealth properties of these nanocapsules could lead to an important accumulation of drugs in accessible sites.

ACKNOWLEDGMENTS

The authors thank O. Lambert for Cryo-TEM studies (UMR-CNRS 5471, Bordeaux, F−33405 France; Université de Bordeaux 1, Bordeaux, F-33405 France). We also want to thank Andréanne Bouchard (University of Technology, Delft, NL-2600 AA The Netherlands) for her valuable comments and suggestions. This work was supported by the departmental committee of Maine-et-Loire of "Ligue contre le cancer."

REFERENCES

1. C. Passirani and J. Benoit. Complement activation by injectable colloidal drug carriers. In R. I. Mahato (ed.), *Biomaterials for Delivery and Targeting of Proteins and Nucleic Acids*, CRC, 2005, pp. 187–230.
2. D. Hoarau, P. Delmas, S. x. E. p. David, E. Roux, and J.-C. Leroux. Novel long-circulating lipid nanocapsules. *Pharm. Res.* **21**:1783–1789 (2004).
3. R. Gref, M. Luck, P. Quellec, M. Marchand, E. Dellacherie, S. Harnisch, T. Blunk, and R. H. Muller. 'Stealth' corona-core nanoparticles surface modified by polyethylene glycol (PEG): influences of the corona (PEG chain length and surface density) and of the core composition on phagocytic uptake and plasma protein adsorption. *Colloids Surf., B Biointerfaces* **18**:301–313 (2000).
4. B. Heurtault, P. Saulnier, B. Pech, J. E. Proust, and J. P. Benoit. Properties of polyethylene glycol 660 12-hydroxy stearate at a triglyceride/water interface. *Int. J. Pharm.* **242**:167–170 (2002).
5. K. Shinoda. The stability of O/W Type Emulsions as Functions of Temperature and the HLB of Emulsifiers: The Emulsification by PIT-Method. *J. Colloid Interface Sci.* **30**:258–263 (1969).
6. T. Tadros, P. Izquierdo, J. Esquena, and C. Solans. Formation and stability of nano-emulsions. *Adv. Colloid Interface Sci.* **108–109**:303–318 (2004).
7. S. Ballot, N. Noiret, F. Hindre, B. Denizot, E. Garin, H. Rajerison, and J. P. Benoit. (99m)Tc/(188)Re-labelled lipid nanocapsules as promising radiotracers for imaging and therapy: formulation and biodistribution. *Eur. J. Nucl. Med. Mol. Imaging* 1–6 (2006).
8. B. Heurtault, P. Saulnier, B. Pech, M.-C. Venier-Julienne, J.-E. Proust, R. Phan-Tan-Luu, and J.-P. Benoit. The influence of lipid nanocapsule composition on their size distribution. *Eur. J. Pharm. Sci.* **18**:55–61 (2003).
9. B.a. Heurtault, P. Saulnier, B. Pech, J.-E. Proust, and J.-P. Benoit. A novel phase inversion-based process for the preparation of lipid nanocarriers. *Pharm. Res.* **19**:875–880 (2002).
10. O. Lambert, N. Cavusoglu, J. Gallay, M. Vincent, J. L. Rigaud, J. P. Henry, and J. Ayala-Sanmartin. Novel organization and properties of annexin 2-membrane complexes. *J. Biol. Chem.* **279**:10872–10882 (2004).
11. G. E. C. Sims and T. J. A. Snope. Method for the estimation of poly(ethylene glycol) in plasma protein fractions. *Anal. Biochem.* **107**:60–63 (1980).
12. H. Ohshima. Dynamic electrophoretic mobility of a soft particle. *J. Colloid Interface Sci.* **233**:142–152 (2001).
13. V. Ducel, P. Saulnier, J. Richard, and F. Boury. Plant protein-polysaccharide interactions in solutions: application of soft particle analysis and light scattering measurements. *Colloids Surf., B Biointerfaces* **41**:95–102 (2005).
14. W. Wang, K. Okamoto, J. Rounds, E. Chambers, and D. O. Jacobs. *In vitro* complement activation favoring soluble C5b-9 complex formation alters myocellular sodium homeostasis. *Surgery* **129**:209–219 (2001).
15. M. T. Peracchia, C. Vauthier, C. Passirani, P. Couvreur, and D. Labarre. Complement consumption by poly(ethylene glycol) in different conformations chemically coupled to poly(isobutyl 2-cyanoacrylate) nanoparticles. *Life Sci.* **61**:749–761 (1997).
16. F. Mevellec, F. Tisato, F. Refosco, A. Roucoux, N. Noiret, H. Patin, and G. Bandoli. Synthesis and characterization of the "sulfur-rich" bis(perthiobenzoato)(dithiobenzoato)technetium(III) heterocomplex. *Inorg. Chem.* **41**:598–601 (2002).
17. J. Allouche, E. Tyrode, V. Sadtler, L. Choplin, and J. L. Salager. Simultaneous conductivity and viscosity measurements as a technique to track emulsion inversion by the phase-inversion-temperature method. *Langmuir* **20**:2134–2140 (2004).
18. W. D. Bancroft. The theory of emulsification. *J. Phys. Chem.***17**: (1913).
19. J. Allouche, E. Tyrode, V. Sadtler, L. Choplin, and J. L. Salager. Single and two steps emulsification to prepare a persistent multiple emulsion with a surfactant-polymer mixture. *Ind. Eng. Chem. Res.* **42**:3982–3988 (2003).
20. S. Marfisi, M. P. Rodriguez, G. Alvarez, M.-T. Celis, A. Forgiarini, J. Lachaise, and J.-L. Salager. Complex emulsion inversion pattern associated with the partitioning of nonionic surfactant mixtures in the presence of alcohol cosurfactant. *Langmuir* **21**:6712–6716 (2005).
21. J. L. Salager, M. Minana-Perez, M. Perez-Sanchez, M. Ramirez-Gouveia, and C. I. Rojas. Surfactant-oil-water systems near the affinity inversion. Part III. The two kinds of emulsion inversion. *J. Dispers. Sci. Technol.* **4**:313–329 (1983).
22. M. C. E. Van Hecke, J. Poprawski, J.-M. Aubry, and J.-L. Salager. A novel criterion for studying the phase equilibria of non-ionic surfactant-triglyceride oil-water systems. *Polym. Int.* **52**:559–562 (2003).
23. J. Poprawski, M. Catte, L. Marquez, M.-J. Marti, J.-L. Salager, and J.-M. Aubry. Application of hydrophilic–lipophilic deviation formulation concept to microemulsions containing pine oil and nonionic surfactant. *Polym. Int.* **52**:629–632 (2003).
24. A. Wadle, T. Forster, and W. Rybinskivon. Influence of the microemulsion phase structure on the phase inversion temperature emulsification of polar oils. *Colloids Surf., A Physicochem. Eng. Asp.* **76**:51–57 (1993).
25. D. Morales, J. M. Gutiérrez, M. J. García-Celma, and Y. C. Solans. A study of the relation between bicontinuous microemulsions and oil/water nano-emulsion formation. *Langmuir* **19**:7196–7200 (2003).
26. A. Vonarbourg, C. Passirani, P. Saulnier, and J. P. Benoit. Evaluation of pegylated lipid nanocapsules *versus* complement system activation and macrophage uptake. *J. Biomed. Mater. Res. A* In Press: (2006).
27. T. Ishida, H. Harashima, and H. Kiwada. Liposome clearance. *Bios. Rep.* **22**:197–224 (2002).
28. H. Harashima, K. Sakata, K. Funato, and H. Kiwada. Enhanced hepatic uptake of liposomes through complement activation depending on the size of liposomes. *Pharm. Res.* **11**:402–406 (1994).
29. S. M. Moghimi and J. Szebeni. Stealth liposomes and long circulating nanoparticles: critical issues in pharmacokinetics, opsonization and protein-binding properties. *Prog. Lipid Res.* **42**:463–478 (2003).
30. S. I. Jeon, J. H. Lee, J. D. Andrade, and P. G. De Gennes. Protein-surface interactions in the presence of polyethylene oxide. I. Simplified theory. *J. Colloid Interface Sci.* **142**:149–158 (1991).

31. I. Minkov, T. Ivanova, I. Panaiotov, J. Proust, and P. Saulnier. Reorganization of lipid nanocapsules at air-water interface. I. Kinetics of surface film formation. *Colloids Surf., B Biointerfaces* **45**:14–23 (2005).
32. V. G. Ivkov and G. N. Berestovskii. Conformation of hydrocarbon chains in a lipid bilayer. *Biofizika* **24**:633–636 (1979).
33. J. M. Smaby, W. J. Baumann, and H. L. Brockman. Lipid structure and the behavior of cholesteryl esters in monolayer and bulk phases. *J. Lipid Res.* **20**:784–788 (1979).
34. M. Vittaz, D. Bazile, G. Spenlehauer, T. Verrecchia, M. Veillard, F. Puisieux, and D. Labarre. Effect of PEO surface density on long-circulating PLA-PEO nanoparticles which are very low complement activators. *Biomaterials* **17**:1575–1581 (1996).
35. A. Vonarbourg, P. Saulnier, C. Passirani, and J. P. Benoit. Electrokinetic properties of noncharged lipid nanocapsules: influence of the dipolar distribution at the interface. *Electrophoresis* **26**:2066–2075 (2005).
36. A. Mori, A. L. Klibanov, V. P. Torchilin, and L. Huang. Influence of the steric barrier activity of amphipathic poly (ethyleneglycol) and ganglioside GM1 on the circulation time of liposomes and on the target binding of immunoliposomes *in vivo*. *FEBS Lett.* **284**:263–266 (1991).
37. R. Gref, Y. Minamitake, M. T. Peracchia, V. Trubetskoy, V. Torchilin, and R. Langer. Biodegradable long-circulating polymeric nanospheres. *Science* **263**:1600–1603 (1994).
38. J.-C. Leroux, E. Allemann, F. De Jaeghere, E. Doelker, and R. Gurny. Biodegradable nanoparticles—from sustained release formulations to improved site specific drug delivery. *J. Control. Release* **39**:339–350 (1996).
39. J.-C. Leroux, F. De Jaeghere, B. Anner, E. Doelker, and R. Gurny. An investigation on the role of plasma and serum opsonins on the internalization of biodegradable poly(D,L-lactic acid) nanoparticles by human monocytes. *Life Sciences* **57**:695–703 (1995).
40. V. C. F. Mosqueira, P. Legrand, J.-L. Morgat, M. Vert, E. Mysiakine, R. Gref, J.-P. Devissaguet, and G. Barratt. Biodistribution of long-circulating PEG-grafted nanocapsules in mice: effects of PEG chain length and density. *Pharm. Res.* **18**:1411–1419 (2001).
41. S. I. Jeon, J. H. Lee, J. D. Andrade, and P. G. De Gennes. Protein-surface interactions in the presence of polyethylene oxide. I. Simplified theory. *J. Colloid Interface Sci.* **142**:149–158 (1991).
42. B. B. Lundberg, B.-C. Mortimer, and T. G. Redgrave. Submicron lipid emulsions containing amphipathic polyethylene glycol for use as drug-carriers with prolonged circulation time. *Int. J. Pharm.* **134**:119–127 (1996).